

Experimental and numerical study of sloshing and swirling in partially filled membrane-type LNG tanks

M. Arai & G.M. Karuka

Yokohama National University, Yokohama, Japan

H. Ando

Monohakobi Technology Institute, Tokyo, Japan

ABSTRACT: In this paper, experimental and numerical studies of sloshing in the prismatic membrane tanks of LNG carriers were carried out. By using partially filled membrane tank models, a series of model experiment was carried out with the motion bed facility. A 3D finite-difference method was used for the numerical simulation and the results were compared with measured ones. In the prismatic shaped membrane tanks, a violent two-dimensional sloshing in the transverse directions of the tanks can easily occur when the tanks are excited at near resonance frequencies. However, in the case if the tank-length-to-tank-breadth ratio is closer to unity, rotational motion of the free surface in the tank, i.e., swirling, may be generated. This phenomenon was further confirmed by a model experiment in a model basin. The conditions that induce the swirling in the prismatic tanks are studied and the tank-length-to-tank-breadth ratio which causes the swirling motion was identified.

1 INTRODUCTION

Liquid cargo tanks of membrane type Liquefied Natural Gas (LNG) carriers have large internal space and if it is partially loaded with the liquid cargo, violent sloshing phenomena may occur in the tanks. Sloshing can cause structural damages of the tank system [e. g., Gavory and de Seze 2009, Lloyd's register 2012] so the classification societies impose a fill range limitation to restrain the occurrence of sloshing. However, in some of the new operational modes such as unloading process of LNG from Floating LNG (FLNG) to shuttle tankers, LNG as fuel for ships, and so on, partial loading is inevitable. Also, partial loading may give ship operators some flexibility in LNG transportation if such loading is acceptable.

In this paper, model experiments and numerical simulations were carried out to examine the sloshing and swirling phenomena in partially filled membrane tanks to make clear the phenomena and obtain criteria for their occurrence.

2 MODEL EXPERIMENTS

In order to examine the hydrodynamic phenomena generated in the tanks of partially filled membrane LNG tanks, we carried out the following two types of model experiments.

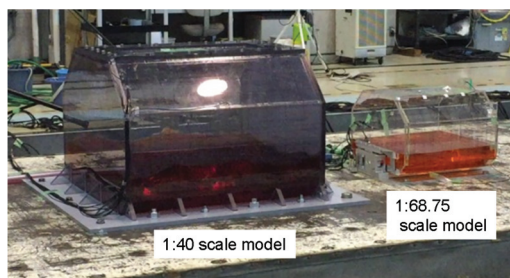


Figure 1. Tank-L (1:40 scale model) and tank-S (1:68.75 scale model) on moving table.

2.1 Sloshing model experiments on a moving table

The first series of model experiments were carried out at MTI Yokohama Laboratory where a 1:40 scale model tank was mounted on a moving table (Figure 1, left). Ten pressure gauges were placed along the walls as shown in Figure 2. The table was excited with regular and irregular sway motions. A smaller model tank of 1:68.75 scale was also used to measure transverse and longitudinal forces acting on the tank (Figure 1, right) by using a two-directional load cell. The configurations of the two tanks are exactly the same and only the tank size were different. Hereafter, we call the former tank as tank-L and the latter as tank-S.

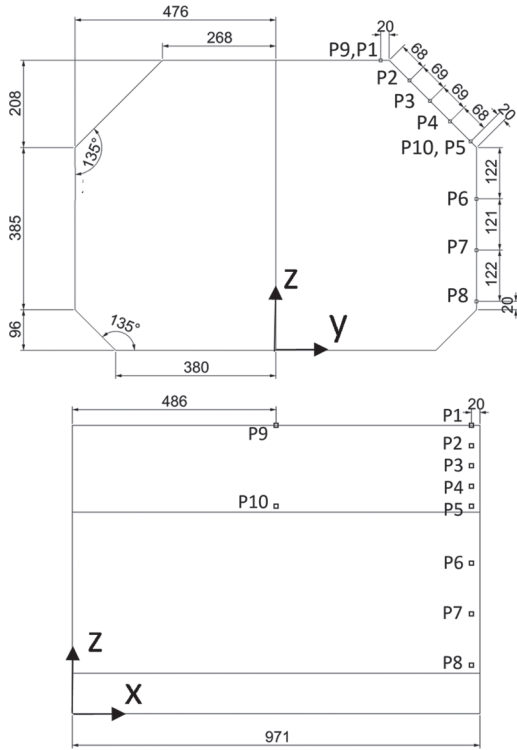


Figure 2. Tank-L (1:40 scale model) and pressure gauge locations (internal tank dimensions are shown in the unit of mm).

2.2 Sloshing model experiment in a model basin

The second series of model experiments were carried out at a model basin of National Maritime Research Institute (NMRI).

Figure 3 and Figure 4 presents the model tank and the LNG carrier model. Tank-S that was used for the model experiment shown in section 2.1 was used in this experiment. As for the liquid cargo in the tank, we used fresh water for the model experiments. Most of recent LNG carriers have four cargo tanks but since the density of LNG is 43% to 47% of that of the fresh water, we installed only two model tanks in the model ship to keep the model ship's draft level to scale correctly the draft of the actual ship. The parameters of the model ship such as the center of gravity of the ship, radius of gyration etc. were also scaled exactly those of the four-tank ship with LNG cargo. The model ship was towed by a moving carriage of the model basin.

Measured items of this model experiment were ship motions, liquid motion in the tanks, tank forces in longitudinal and lateral directions and pressure at 3 locations in the fore tank.

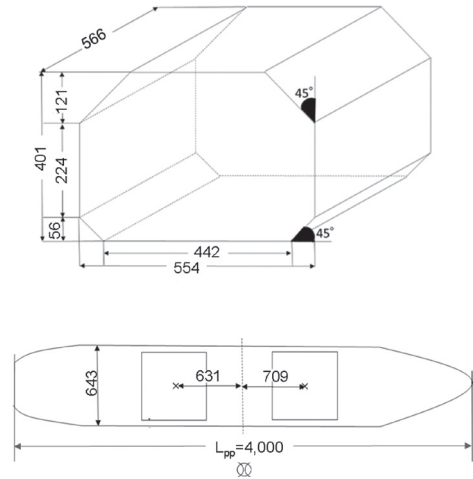


Figure 3. Tank-S (1:68.75 scale model) and model ship.

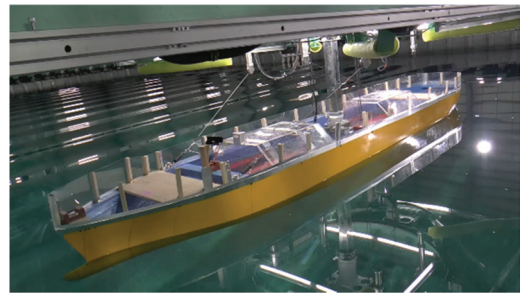


Figure 4. Setup of model tanks and model ship.

3 NUMERICAL METHOD

The numerical method used in the analysis of sloshing was based on the finite difference technique developed by the authors (Arai, Cheng, Kumano & Miyamoto 2002) for partial load conditions. The numerical method is outlined below.

The flow field in the tank is assumed to be three-dimensional, and the fluid is assumed to be incompressible and inviscid. The governing equations in the Cartesian coordinate system (x, y, z) fixed to the tank are the mass continuity equation:

$$\frac{\partial u}{\partial x} + \frac{\partial v}{\partial y} + \frac{\partial w}{\partial z} = 0 \quad (1)$$

and Euler's equations of motion:

$$\frac{\partial u}{\partial t} + u \frac{\partial u}{\partial x} + v \frac{\partial u}{\partial y} + w \frac{\partial u}{\partial z} = -\frac{1}{\rho} \cdot \frac{\partial p}{\partial x} + f_x \quad (2)$$

$$\frac{\partial v}{\partial t} + u \frac{\partial v}{\partial x} + v \frac{\partial v}{\partial y} + w \frac{\partial v}{\partial z} = -\frac{1}{\rho} \cdot \frac{\partial p}{\partial y} + f_y \quad (3)$$

$$\frac{\partial w}{\partial t} + u \frac{\partial w}{\partial x} + v \frac{\partial w}{\partial y} + w \frac{\partial w}{\partial z} = -\frac{1}{\rho} \cdot \frac{\partial p}{\partial z} + f_z \quad (4)$$

in which the variables are defined as follows:

u, v, w : components of the velocity in the x, y and z directions, respectively,

ρ : liquid density,

p : pressure,

f_x, f_y, f_z : external forces in the x, y and z directions, respectively.

The change of the free surface of the fluid over time was calculated by the following equation:

$$\frac{\partial H}{\partial t} + u \frac{\partial H}{\partial x} + v \frac{\partial H}{\partial y} = w \quad (4)$$

where $H = H(t, x, y)$ is the vertical position of the free surface. This simplified expression of the free surface cannot treat an extremely local deformation of the free surface such as spray. However, the present method has an excellent feature of numerically stable computation and also it can simulate the violent flow in the tank including the impact of the liquid on the tank ceiling (Arai et al. 2002, 2006a, 2006b).

4 RESULTS OF THE MODEL EXPERIMENTS AND NUMERICAL SIMULATION

4.1 Responses by regular excitation

In this section, model test results when we applied regular sway motion to the tank will be shown. Figure 5 and Figure 6 show the computed and experimentally recorded liquid motion of 50% filling case when we applied a regular sway motion with the excitation frequency coincided with the natural frequency of the liquid motion inside the tank. At the beginning of the test, almost two-dimensional free surface motion in the lateral direction was observed (Figure 5). However, after a period of time, the free surface started to rotate in the tank as shown in Figure 6. This rotating motion is called swirling and it is often observed in axisymmetric tanks such as spherical or vertically placed cylindrical ones. In our model tests we used a prismatic tank whose tank breadth and tank length were almost the same and this might have caused the generation of the swirling.

In the case of 30% filling level, the situation was almost the same as that of 50%. In the case of the liquid level more than 70%, however, only 2-dimensional sloshing was observed, because the

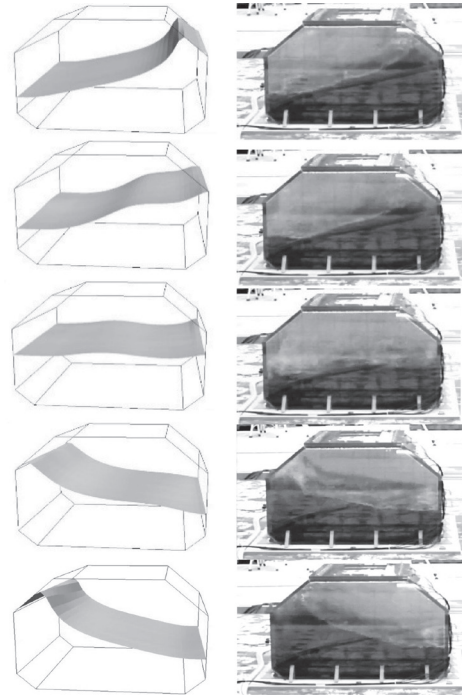


Figure 5. Liquid motion in sloshing phase.

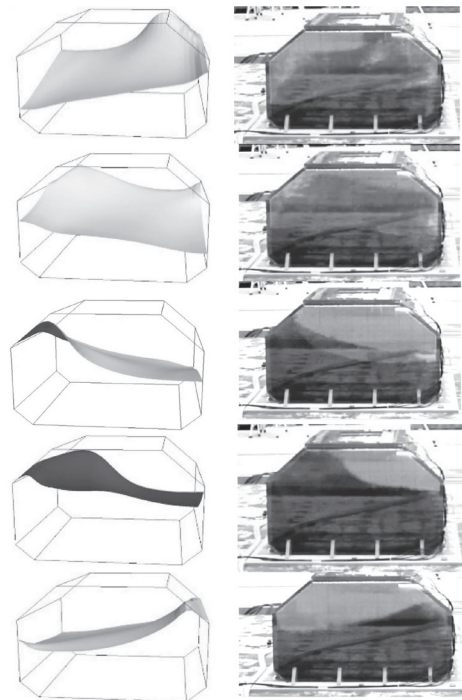


Figure 6. Liquid motion in swirling phase.

free-surface area was limited by the top chamfers and swirling motion was difficult to occur.

Figure 7 shows an example of the computed force time histories. Regular sway motion was applied to the tank. F_y is the computed lateral force component, and F_x is the longitudinal force component. As an initial condition of the numerical simulation, a small inclination (i.e., 1 degree) was given to the free surface to generate the swirling motion. This small initial disturbance was necessary since it was difficult to generate the swirling motion in the numerical simulation without it. At the beginning of the simulation, only F_y was generated as shown in Figure 7 but after some period of time, swirling motion started and the amplitude of F_x increased to be almost the same as that of F_y .

Figure 8 presents snapshots of pressure distribution obtained by the numerical simulation in the tank with 50% filling case. Pressure distributions in the sloshing phase are shown. The left figure shows the total pressure and the right figure shows the dynamic pressure. Here, in our study, the dynamic pressure was estimated by subtracting the static pressure from the total pressure. It is easy to see the effect of sloshing by this dynamic pressure representation. Figure 9 presents the dynamic pressure distribution in the swirling phase.

Figure 10 shows the maximum pressure distribution in the whole simulation period of the 50%

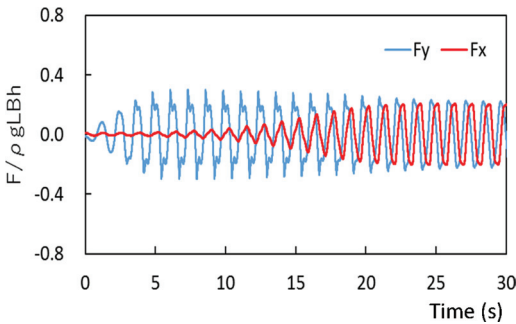


Figure 7. A typical result of computed force histories.

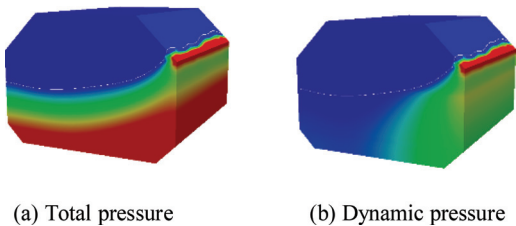


Figure 8. Pressure distribution (sloshing phase, snap shots).

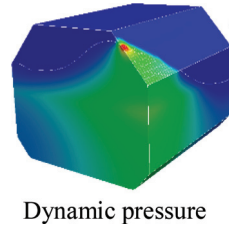


Figure 9. Pressure distribution (swirling phase, snap shot).

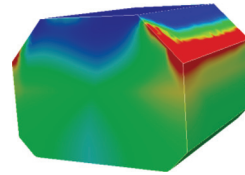


Figure 10. Maximum dynamic pressure distribution (50% filling).

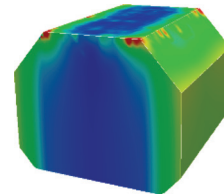


Figure 11. Maximum dynamic pressure distribution (95% filling).

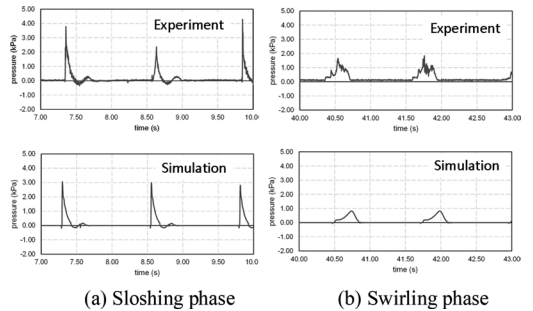


Figure 12. Comparison between computed and measured pressure histories (tank-L, P-5, 50% filling level, $f = 0.804$ Hz).

filling case. Sloshing causes high pressure at the lower end of the top chamfer, and the swirling causes the high pressure distribution at the connecting part of the end plate and the top chamfer. Figure 10 presents the super position of pressure generated in these two phases.

Figure 11 presents the maximum pressure distribution of the 95% filling case. High pressure zone is limited at the top corner of the tank and the magnitude of the impact pressure is lower than that of 50% filling case.

Figure 12 compares measured and computed pressure time histories at the lower part of the chamfer (P5, see Figure 2). Our numerical method can simulate pressure histories both in sloshing and swirling phases.

4.2 Results obtained by the tests at model basin

In this section, we will show two examples of the test results obtained at the model basin. Model tank setup in the model ship has been already shown in section 2.2 (Figure 3).

The first test case was the one when the wave encounter period was almost the same as that of the natural period of the ship's roll motion. Wave encounter angle was 90 degrees, i.e., beam sea. In this case, ship motion was large but the internal liquid motion was mild. Only the force in the tank's lateral direction (F_y) was large.

On the other hand, Figure 14 shows the case when the wave encounter period was almost the same as the natural period of the tank-liquid motion. In this case, not only F_y but also F_x became large and we could see the generation of swirling.

An interesting phenomenon is that the force histories shown in Figure 14 has four stages. First, sloshing occurred (stage A) but gradually the free surface started to rotate (stage B). Then the motion became small (stage C) and the rotation started again (stage D) but this time the rotating direction was opposite to the stage A.

Figure 15 presents RAOs of the lateral and longitudinal force components measured by the

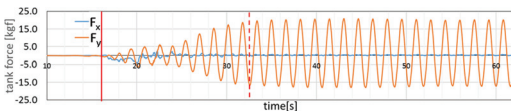


Figure 13. Measured force histories by model basin experiment (encounter wave period is at the natural period of ship roll motion).

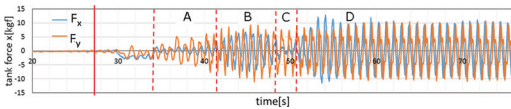


Figure 14. Measured force histories by model basin experiment (encounter wave period is at the natural period of tank liquid motion).

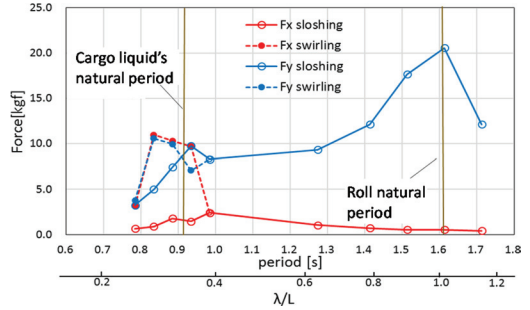


Figure 15. Relation between RAO of liquid surface motion and frequency of sea waves.

model experiments. As for the lateral force (F_y), we observed two peaks. The right peak appeared when the encounter period coincided the natural period of ship's roll motion. Since the fluid motion in the tank was almost two dimensional in the ship's lateral direction, only F_y appeared and F_x was almost zero. When the wave encounter period became close to the tank liquid's natural period, violent liquid motion was generated and second peak of F_y appeared. As shown in Figure 14, sometimes two-dimensional sloshing motion occurred first and swirling motion followed. Therefore in Figure 15, the values when sloshing was generated were shown by solid lines, and when swirling occurred the RAOs of F_x and F_y were shown by dotted lines. Swirling phenomena was significant when the encounter wave period was slightly lower than the internal liquid's natural period which could be observed by the increase of F_x at such periods.

5 DISCUSSION ON SWIRLING PHENOMENA

5.1 Condition for swirling generation

As shown in Figure 7 and Figure 14, in some test cases, two-dimensional sloshing motion occurred in the beginning of the model tests but it transferred to swirling motion later. We considered that the swirling motion related to the tank shape, therefore in this section, we computed the force histories for different tank length (L) to tank breadth (B) ratio (i.e., L/B).

As presented in Figure 7, the occurrence of the swirling was easily distinguished by the emergence of the longitudinal force (F_x). In this study the tank breadth was kept constant and the tank length was changed for several cases and the computed results were examined. The tanks were excited with a regular sway excitation with 20 mm amplitude at the natural sloshing period. Examples of the computed

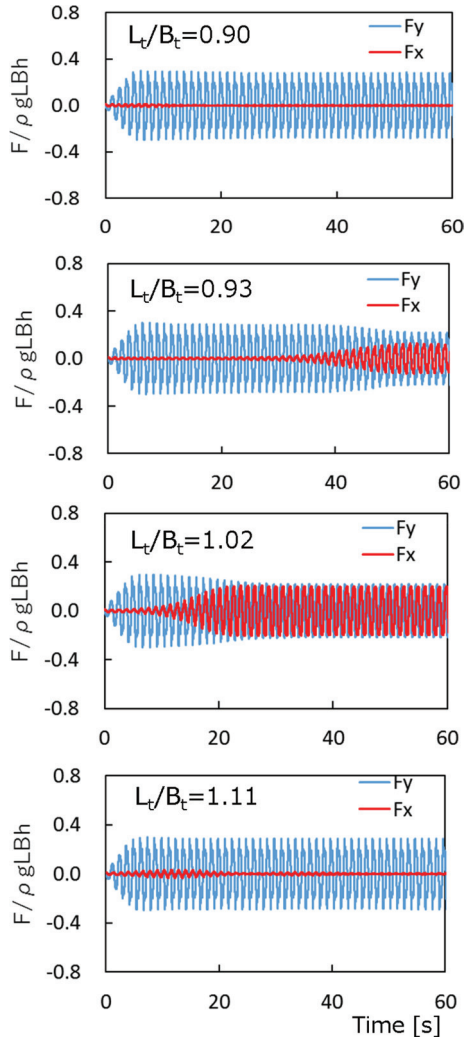


Figure 16. Comparison of F_x and F_y for different L_t/B_t ratios (50% filling level).

histories of the force components are shown in Figure 16. Figure 17 and Figure 18 summarize the computed F_x/F_y ratio for tanks with different L_t/B_t for two conditions, 30% and 50% filling levels, respectively. It can be clearly seen that the swirling occurred with high intensity when L_t/B_t ratio was near 1. For both cases swirling occurred in a range $0.9 < L_t/B_t < 1.10$. As for the filling level, we observed that swirling occurred when filling level was 30% to 60%.

5.2 Actual LNG ships' tank dimensions

We examined the tank dimensions of 14 constructed or designed membrane-type LNG carriers,

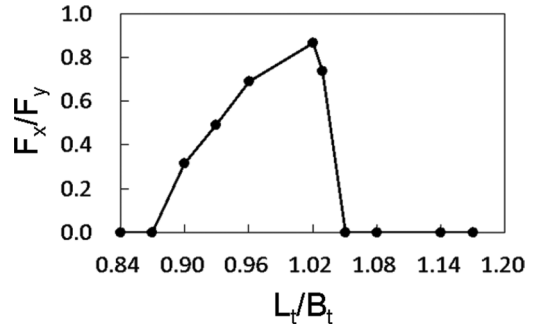


Figure 17. Computed F_x/F_y for different L_t/B_t ratio (30% filling level).

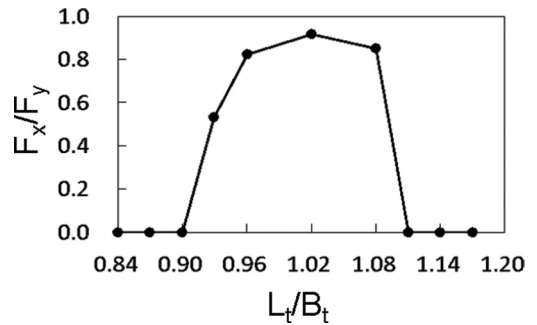


Figure 18. Computed F_x/F_y for different L_t/B_t ratio (50% filling level).

Table 1. Tank length to breadth (L_t/B_t) ratio of actual or designed ships which has L_t/B_t between 0.9 and 1.1.

Ship ID	No.4 Tank		No.3 Tank		No.2 Tank		No.1 Tank					
	L_t (m)	B_t (m)	L_t/B_t	B_t (m)	L_t/B_t	L_t (m)	B_t (m)	L_t/B_t				
1	46.05	42.65	1.08	46.05	42.65	1.08	46.05	42.65	1.08	31.09	36.53	0.85
2	40.00	37.81	1.06	44.75	37.81	1.18	44.75	37.81	1.18	31.45	33.75	0.93
3	47.07	41.63	1.13	47.07	41.63	1.13	47.07	41.63	1.13	33.81	32.11	1.05
4	49.60	49.90	0.99	49.60	49.90	0.99	49.60	49.90	0.99	Wedge shape		
5	38.38	37.81	1.02	43.58	37.81	1.15	43.89	37.81	1.16	Wedge shape		

and 5 of them had the tanks that met above mentioned criteria (i.e., $0.9 < L_t/B_t < 1.10$). Table 1 presents those ships. If the liquid cargo is partially loaded in the tanks swirling is expected to occur.

5.3 Possibility of the occurrence of swirling in actual irregular seaways

The next question is “does swirling really occur in the actual irregular seaways?”, since the actual encounter waves are irregularly changes in time.

In order to study this, we excited the model tank (Tank-S) on a moving table shown in Figure 1 with irregular sway motions. Time histories of

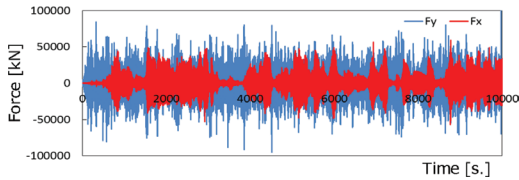


Figure 19. Measured force histories by a moving table model experiment (irregular sway motion, $H_{1/3} = 5.89$ m, $T_{mean} = 9.55$ s in actual ship scale).

the tank's sway motion was prepared by using the typical wave spectrum data and ship's sway motion RAO. The measured time histories of F_x and F_y are shown in Figure 19. We can judge that the swirling is occurring if the magnitude of F_x becomes large. From Figure 19 we can conclude that swirling is generated by the irregular tank motion which simulates the actual seaways.

6 CONCLUSIONS

In this study a series of simulations for different filling levels were carried out and compared with experimental data.

- The general fluid motion and dynamic pressures obtained by our numerical sloshing simulation agree well with experimental data, which confirms the suitability of the numerical tool to represent the phenomena.
- For middle to low filling levels, swirling occurs if the tank length to breadth ratio is near 1.0. On the other hand swirling does not appear in high filling conditions, i.e., 70% or more filling levels. We also confirmed that swirling in membrane tanks can occur in the actual irregular seaways.
- In partially loaded conditions, very complicated liquid motion in the tank is generated when the encounter wave period is near the natural period of the tank liquid motion. For other encounter periods, the liquid motion in the tank is almost two dimensional and the wave inside the tank is generated almost parallel to the tank walls.

ACKNOWLEDGEMENTS

The authors would like to thank Mr. H. Miyazaki for the support of the model experiment at the

Actual Sea Model Basin of the National Maritime Research Institute. Part of this research was carried out as ClassNK's Joint R&D with industries and Academic Partners Project.

REFERENCES

- Abramson, H. M., Bass R. L., Faltinsen, O., Olsen, HA. 1974. Liquid Slosh in LNG Carriers, 10th Naval Hydro-Dynamics Symposium, 21–38.
- Arai, M., Cheng, L.Y., Kumano, A., Miyamoto, T. 2002. A Technique for Stable Numerical Computation of Hydrodynamic Impact Pressure in Sloshing Simulation, Journal of the Society of Naval Architects of Japan, Vol. 191, 299–307.
- Arai, M., Makiyama, H.S., Cheng, L.Y., Kumano, A., Ando, T. 2006. Numerical and Experimental Study of 3-D Sloshing in Tanks of LNG Carriers, Proceedings of OMAE 2006, Paper No. OMAE 2006-92235.
- Arai M., Makiyama, H.S., Cheng, L.Y., Kumano, A., Ando, T., Imakita, A. 2006. Numerical Analysis of 3-D Sloshing In Tanks of Membrane-Type LNG Carriers, ICSOT 2006, Design, Construction & Operation of Natural Gas Carriers & Offshore Systems, 201–209.
- Arai, M, Bogaert, H., Graczyk, M., Ha, M.K., Kim, W.S., Lindgren, M., Martin, E., Noble, P., Tao, L., Valle, O., Xiong, Y. 2012. Report of Committee V.2, Natural Gas Storage and Transportation, Proceedings of 18th International Ship and Offshore Structures Congress, Volume 2, 67–112.
- Arai M., Cheng L.Y., Wang X., Okamoto N., Hata R., Gustavo M.K. 2016. Sloshing and swirling behavior of liquid in a spherical LNG tank, Proceedings of International Symposium on Ships and Other Floating Structures PRADS 2016.
- Cheng, L.Y., Arai, M. 2005. A 3D Numerical Method for Assessment of Impact Loads Due to Sloshing in Liquid Cargo Tanks, Proceedings of the Fifteenth International Offshore and Polar Engineering Conference, 214–221.
- Faltisen, O.M., Timokha A.N. 2013. Nonlinear sloshing in a spherical tank, Conference Proceedings of OMAE 2013, Paper No. OMAE 2013-10036.
- Gavory T., de Seze, P.E. 2009. Sloshing in membrane LNG carriers and its consequences from a designer's perspective, Conference Proceedings of ISOPE 2009, Paper No. 2009-FD-11.
- Gustavo M.K., Arai, M., Ando, H. 2017. Sloshing and Swirling in Partially Loaded Prismatic Tanks, OMAE 2017-61562.
- Lloyd's Register, 2012. Guidance on the Operation of Membrane LNG Ships to Reduce the Risk of Damage due to Sloshing.